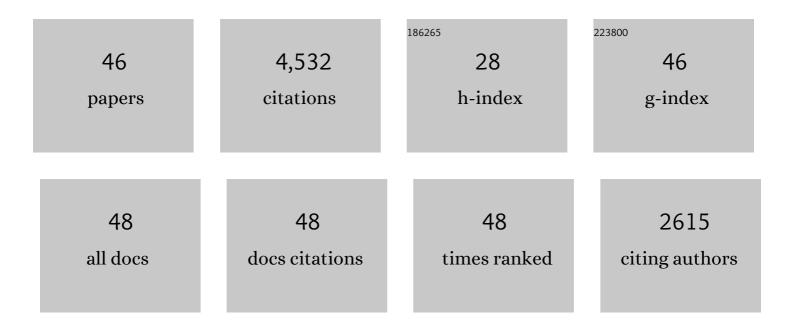
Brian Kendall

List of Publications by Year in descending order

Source: https://exaly.com/author-pdf/6661074/publications.pdf Version: 2024-02-01



#	Article	IF	CITATIONS
1	A Whiff of Oxygen Before the Great Oxidation Event?. Science, 2007, 317, 1903-1906.	12.6	822
2	Ocean oxygenation in the wake of the Marinoan glaciation. Nature, 2012, 489, 546-549.	27.8	420
3	Re-Os geochronology of postglacial black shales in Australia: Constraints on the timing of "Sturtian― glaciation. Geology, 2006, 34, 729.	4.4	250
4	Oceanic oxygenation events in the anoxic Ediacaran ocean. Geobiology, 2016, 14, 457-468.	2.4	241
5	Pervasive oxygenation along late Archaean ocean margins. Nature Geoscience, 2010, 3, 647-652.	12.9	233
6	Uranium and molybdenum isotope evidence for an episode of widespread ocean oxygenation during the late Ediacaran Period. Geochimica Et Cosmochimica Acta, 2015, 156, 173-193.	3.9	222
7	Re–Os and Mo isotope systematics of black shales from the Middle Proterozoic Velkerri and Wollogorang Formations, McArthur Basin, northern Australia. Geochimica Et Cosmochimica Acta, 2009, 73, 2534-2558.	3.9	209
8	THE STABLE ISOTOPE GEOCHEMISTRY OF MOLYBDENUM. Reviews in Mineralogy and Geochemistry, 2017, 82, 683-732.	4.8	191
9	Constraints on the timing of Marinoan "Snowball Earth―glaciation by 187Re–187Os dating of a Neoproterozoic, post-glacial black shale in Western Canada. Earth and Planetary Science Letters, 2004, 222, 729-740.	4.4	155
10	Molybdenum isotope evidence for mild environmental oxygenation before the Great Oxidation Event. Geochimica Et Cosmochimica Acta, 2010, 74, 6655-6668.	3.9	139
11	Trace elements at the intersection of marine biological and geochemical evolution. Earth-Science Reviews, 2016, 163, 323-348.	9.1	135
12	Extensive marine anoxia during the terminal Ediacaran Period. Science Advances, 2018, 4, eaan8983.	10.3	126
13	Uranium isotope fractionation suggests oxidative uranium mobilization at 2.50 Ga. Chemical Geology, 2013, 362, 105-114.	3.3	101
14	Molybdenum isotope constraints on the extent of late Paleoproterozoic ocean euxinia. Earth and Planetary Science Letters, 2011, 307, 450-460.	4.4	99
15	Fully oxygenated water columns over continental shelves before the Great Oxidation Event. Nature Geoscience, 2019, 12, 186-191.	12.9	95
16	Bioavailability of zinc in marine systems through time. Nature Geoscience, 2013, 6, 125-128.	12.9	84
17	Oxygenation of a Cryogenian ocean (Nanhua Basin, South China) revealed by pyrite Fe isotope compositions. Earth and Planetary Science Letters, 2015, 429, 11-19.	4.4	80
18	Global correlation of the Vazante Group, São Francisco Basin, Brazil: Re–Os and U–Pb radiometric age constraints. Precambrian Research, 2008, 164, 160-172.	2.7	70

BRIAN KENDALL

#	Article	IF	CITATIONS
19	A model for the oceanic mass balance of rhenium and implications for the extent of Proterozoic ocean anoxia. Geochimica Et Cosmochimica Acta, 2018, 227, 75-95.	3.9	66
20	¹⁸⁷ Re- ¹⁸⁷ Os geochronology of Precambrian organic-rich sedimentary rocks. Geological Society Special Publication, 2009, 326, 85-107.	1.3	65
21	Correlation of Sturtian diamictite successions in southern Australia and northwestern Tasmania by Re–Os black shale geochronology and the ambiguity of "Sturtian―type diamictite–cap carbonate pairs as chronostratigraphic marker horizons. Precambrian Research, 2009, 172, 301-310.	2.7	65
22	Transient episodes of mild environmental oxygenation and oxidative continental weathering during the late Archean. Science Advances, 2015, 1, e1500777.	10.3	61
23	Uranium isotope compositions of mid-Proterozoic black shales: Evidence for an episode of increased ocean oxygenation at 1.36 Ga and evaluation of the effect of post-depositional hydrothermal fluid flow. Precambrian Research, 2017, 298, 187-201.	2.7	61
24	Multiple negative molybdenum isotope excursions in the Doushantuo Formation (South China) fingerprint complex redox-related processes in the Ediacaran Nanhua Basin. Geochimica Et Cosmochimica Acta, 2019, 261, 191-209.	3.9	52
25	Anomalous molybdenum isotope trends in Upper Pennsylvanian euxinic facies: Significance for use of Î′98Mo as a global marine redox proxy. Chemical Geology, 2012, 324-325, 87-98.	3.3	48
26	Re–Os age constraints and new observations of Proterozoic glacial deposits in the Vazante Group, Brazil. Precambrian Research, 2013, 238, 199-213.	2.7	48
27	Marine redox conditions during deposition of Late Ordovician and Early Silurian organic-rich mudrocks in the Siljan ring district, central Sweden. Chemical Geology, 2017, 457, 75-94.	3.3	42
28	Redox conditions across the Cambrian–Ordovician boundary: Elemental and isotopic signatures retained in the GSSP carbonates. Palaeogeography, Palaeoclimatology, Palaeoecology, 2015, 440, 440-454.	2.3	33
29	Inverse correlation between the molybdenum and uranium isotope compositions of Upper Devonian black shales caused by changes in local depositional conditions rather than global ocean redox variations. Geochimica Et Cosmochimica Acta, 2020, 287, 141-164.	3.9	29
30	Estimating ancient seawater isotope compositions and global ocean redox conditions by coupling the molybdenum and uranium isotope systems of euxinic organic-rich mudrocks. Geochimica Et Cosmochimica Acta, 2020, 290, 76-103.	3.9	27
31	Recent Advances in Geochemical Paleo-Oxybarometers. Annual Review of Earth and Planetary Sciences, 2021, 49, 399-433.	11.0	25
32	Depositional age of the early Paleoproterozoic Klipputs Member, Nelani Formation (Ghaap Group,) Tj ETQq0 0 0 r Paleoproterozoic global correlations. Precambrian Research, 2013, 237, 1-12.	gBT /Over 2.7	lock 10 Tf 50 24
33	Genesis of a giant Paleoproterozoic strata-bound magnesite deposit: Constraints from Mg isotopes. Precambrian Research, 2016, 281, 673-683.	2.7	23
34	Molybdenum isotope-based redox deviation driven by continental margin euxinia during the early Cambrian. Geochimica Et Cosmochimica Acta, 2022, 325, 152-169.	3.9	23
35	Temporal record of osmium concentrations and 187Os/188Os in organic-rich mudrocks: Implications for the osmium geochemical cycle and the use of osmium as a paleoceanographic tracer. Geochimica Et Cosmochimica Acta, 2017, 216, 221-241.	3.9	22
36	A multi-isotope approach towards constraining the origin of large-scale Paleoproterozoic B-(Fe) mineralization in NE China. Precambrian Research, 2017, 292, 115-129.	2.7	15

BRIAN KENDALL

#	Article	IF	CITATIONS
37	An expanded shale Î'98Mo record permits recurrent shallow marine oxygenation during the Neoarchean. Chemical Geology, 2020, 532, 119391.	3.3	15
38	Molybdenum Isotope Constraints on the Origin of Vanadium Hyper-Enrichments in Ediacaran–Phanerozoic Marine Mudrocks. Minerals (Basel, Switzerland), 2020, 10, 1075.	2.0	13
39	The Mo- and U-isotope signatures in alternating shales and carbonate beds of rhythmites: A comparison and implications for redox conditions across the Cambrian-Ordovician boundary. Chemical Geology, 2022, 602, 120882.	3.3	10
40	16 Good Golly, Why Moly? THE STABLE ISOTOPE GEOCHEMISTRY OF MOLYBDENUM. , 2017, , 683-732.		9
41	An osmium-based method for assessing the source of dissolved rhenium and molybdenum to Archean seawater. Chemical Geology, 2014, 385, 92-103.	3.3	6
42	New constraints on mid-Proterozoic ocean redox from stable thallium isotope systematics of black shales. Geochimica Et Cosmochimica Acta, 2021, 315, 185-206.	3.9	6
43	Significance of 56Fe depletions in late-Archean shales and pyrite. Geochimica Et Cosmochimica Acta, 2022, 316, 87-104.	3.9	6
44	Consecutive Fe redox cycles decrease bioreducible Fe(III) and Fe isotope fractionations by eliminating small clay particles. Geochimica Et Cosmochimica Acta, 2021, 308, 118-135.	3.9	4
45	Shale Heavy Metal Isotope Records of Low Environmental O2 Between Two Archean Oxidation Events. Frontiers in Earth Science, 2022, 10, .	1.8	4
46	Insights from modern diffuse-flow hydrothermal systems into the origin of post-GOE deep-water Fe-Si precipitates. Geochimica Et Cosmochimica Acta, 2022, 317, 1-17.	3.9	2